DOI: 10.1002/ejic.200900110

Anion–π, Lone-Pair–π, π–π and Hydrogen-Bonding Interactions in a Cu^{II} Complex of 2-Picolinate and Protonated 4,4′-Bipyridine: Crystal Structure and Theoretical Studies

Chaitali Biswas,[a,b] Michael G. B. Drew,[c] Daniel Escudero,[d] Antonio Frontera,*[d] and Ashutosh Ghosh*[a]

Keywords: Ab initio calculations / Noncovalent interactions / Hydrogen bonds / Copper / Pi interactions

A Cu^{II} complex of protonated 4,4′-bipyridine (Hbyp) and 2-picolinate (pic), $[Cu_2(pic)_3(Hbyp)(H_2O)(ClO_4)_2]$, has been synthesised and characterised by single-crystal X-ray analysis. The structure consists of two copper atoms that have different environments, bridged by a carboxylate group. The equatorial plane is formed by the two bidentate picolinate groups in one Cu^{II}, and one picolinate, one monodentate 4,4′-bipyridyl ligand and a water molecule in the other. Each copper atom is also weakly bonded to a perchlorate anion in an axial position. One of the coordinated perchlorate groups displays anion–π interaction with the coordinated pyridine ring. The noncoordinated carboxylate oxygen is involved in lone-pair (l.p.)–π interaction with the protonated pyridine ring. In addition there are π–π and H-bonding interactions in the structure. Bader's theory of "atoms in molecules" (AIM) is used to characterise the anion–π and l.p.–π interactions observed in the solid state. A high-level ab initio study (RI-MP2/aug-cc-pVTZ level of theory) has been performed to analyse the anion–π binding affinity of the pyridine ring when it is coordinated to a transition metal and also when the other pyridine ring of the 4,4′-bipyridine moiety is protonated. Theoretical investigations support the experimental findings of an intricate network of intermolecular interactions, which is characterised in the studied complex, and also indicate that protonation as well as coordination to the transition metal have important roles in influencing the π-binding properties of the aromatic ring.

Introduction

Noncovalent interactions between molecules are weak intermolecular contacts that play a pivotal role in biological systems and govern the physicochemical properties of molecular systems in the condensed phase.[1] Noncovalent binding interactions are nowadays commonly used for the self-assembly of large supramolecular aggregates in solution with specific chemical properties.[2] Supramolecular interactions of aromatic systems have attracted considerable attention during the past few years[3] because the utilisation of intermolecular noncovalent interactions is relied upon for the design and development of functional materials. Noncovalent interactions form the backbone of supramolecular chemistry and include hydrogen bond, stacking, electrostatic, hydrophobic and charge-transfer interactions as well as metal ion coordination.[4] C–H···π and cation···π contacts are well-established supramolecular interactions[5] and numerous crystallographic examples are regularly reported. In the recent past, a new type of noncovalent supramolecular interaction involving aromatic molecules has been considered, namely, the binding association between an anion and an electron-deficient π-ring,[6] or even between a lone pair and an electron-deficient aromatic ring.[7] Some experimental and extensive theoretical studies have confirmed that π-acidic systems as diverse as halo-,[8] nitro- and cyano-substituted benzenes,[9] calixarenes,[10] cyanuric acids,[11] tetrazines[12] and triazines[13] can interact with simple anions such as halides or more charge delocalised multiatomic anions such as NO_3^-, ClO_4^- and BF_4^- as well as with neutral lone-pair donor atoms such as nitrogen and oxygen. If anion–π or lone-pair–π interactions are to be exploited in synthetic anion receptors, it is necessary to design systems incorporating sufficient π-acidity. Metal–ligand interactions involving heterocyclic rings based on triazine and tetrazine have already shown potential in this area. The presence of a number of heteroatoms perturbs the π-electron density of the ring, which is further polarised upon coordination to a positively charged metal ion.[3] In addition, if the ring can potentially bridge between metal ions,

[a] Department of Chemistry, University College of Science, University of Calcutta,
92 A. P. C. Road, Kolkata 700009, India
E-mail: ghosh_59@yahoo.com
[b] Sarojini Naidu College for Women,
30 Jessore Road, Kolkata 700028, India
[c] School of Chemistry, The University of Reading,
P. O. Box 224, Whiteknights, Reading RG6 6AD, UK
[d] Departament de Química, Universitat de les Illes Balears,
Crta. de Valldemossa km 7.5, 07122 Palma de Mallorca, Baleares, Spain
E-mail: toni.frontera@uib.es

a more π-acidic heterocyclic ring centre will result. Coordination polymer systems are likely to be useful in this respect. However, a subtle balance is required between electron deficiency and donor ability because electron-deficient heterocycles such as triazines and tetrazines are weak donors and, as a result, are more inclined to form discrete complexes. One of the challenges in this area is to design appropriate chemical systems incorporating sufficient π-acidity apart from electron-deficient heterocycles such as triazine and tetrazine donors. In most cases, simple metal complexes will not provide sufficient polarisation to produce strong anion–π or lone-pair–π binding. On the other hand, ab initio calculations have provided evidence that these weak interactions can afford a significant degree of stability if the aromatic moiety is protonated.[14] However, it is very difficult to synthesise a system in which a protonated heterocyclic base is coordinated to a metal ion and to obtain such system at least two donor sites in the base are needed so that one is coordinated and the other is protonated. It is even more challenging to synthesise a metal complex that shows anion–π, lone-pair–π and π–π interactions simultaneously, as for the former two interactions electron-deficient π-systems are required but for the last one electron-rich π-systems are required.

In order to realise such a system, we succeeded in synthesising a Cu^{II} complex of protonated 4,4′-bipyridine, $[Cu_2(pic)_3(Hbyp)(H_2O)(ClO_4)_2]$ (**1**) (pic = 2-picolinate, byp = 4,4′-bipyridine), which is characterised by single-crystal X-ray analysis. As anticipated, the electron-deficient Hbyp moiety participates in anion–π and lone-pair–π interactions and the electron-rich 2-picolinate ligand is involved in π–π interactions. The observed anion–π, lone-pair–π and π–π interactions along with hydrogen bonds form the 3D network in the structure. We have used Bader's theory of "atoms in molecules" (AIM) to characterise the anion–π and l.p.–π interactions observed in the solid state. The AIM theory has been successfully used to characterise a great variety of interactions and provides an unambiguous definition of chemical bonding.[15] We have also performed a high-level ab initio study (RI-MP2/aug-cc-pVTZ level of theory) on a model of the crystal structure where we analyse the influence of two factors on the π-binding ability of one pyridine ring belonging to a 4,4′-bipyridine molecule. The study shows how the anion–π binding affinity of the pyridine ring is affected when it is coordinated to a transition metal and how it is then subsequently affected when the other pyridine ring of the 4,4′-bipyridine moiety is protonated.

Results and Discussion

The complex $[Cu_2(pic)_3(Hbyp)(H_2O)(ClO_4)_2]$ (**1**) is easily obtained by the reaction of 3 equiv. of picolinic acid with 2 equiv. of $Cu(ClO_4)_2{\cdot}6H_2O$ and 1 equiv. of 4,4′-bipyridine, in the presence of perchloric acid, which was added to bring the pH to about 2. Initially a small amount of bis(2-picolinate)copper(II) dihydrate separated out. It was filtered off. The desired compound was separated as a crystalline solid on keeping the filtrate at room temperature for several days. Complex **1** possesses all functional groups required to favour their supramolecular self-assembly through the simultaneous occurrence of H-bond, π–π, anion–π and l.p.–π interactions. It contains C=O bonds (in which the O atom contains an electron lone-pair), electron-rich π-rings (picolinate pyridine ring), electron-poor π-rings (protonated bipyridine ring) and electron-rich perchlorate anions (Scheme 1).

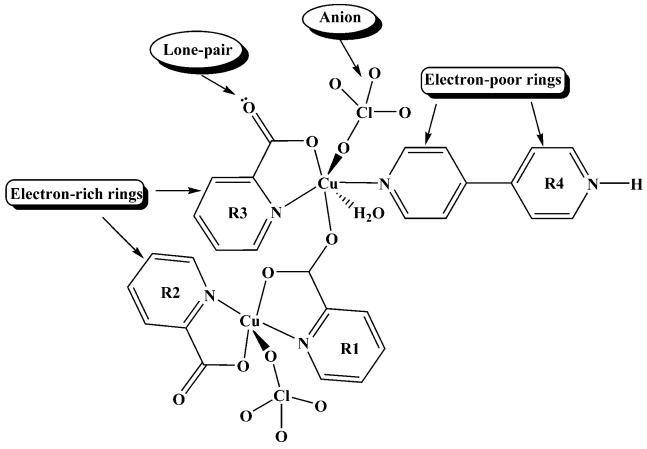

Scheme 1. Representation of compound **1**, showing the functional groups that can be involved in supramolecular interactions.

Description of the Structures of $[Cu_2(pic)_3(Hbyp)(H_2O)(ClO_4)_2]$ (1)

The crystal structure of **1** is depicted in Figure 1 together with the numbering scheme in the metal coordination spheres. The bond lengths and angles are listed in Table 1. The structure of **1** contains two copper atoms with different environments. Cu(1) is bonded to two bidentate picolinates by a nitrogen atom of the pyridine ring at 1.966(5), 1.979(4) Å and an oxygen atom of the carboxylate group at 1.947(4), 1.977(4) Å. This N2O2 equatorial plane is slightly distorted with an r.m.s. of 0.101 Å. Cu(1) is 0.024(2) Å from the plane. There is a perchlorate oxygen atom O(81) in an axial position at 2.546(4) Å. In the other axial position is the coordinated oxygen atom of the carboxylate, O(28) (1 – *x*, –*y*, –*z*) at 2.835(5) Å, but this is not considered to represent a bonding interaction. By contrast Cu(2) is bonded to one bidentate picolinate with bond lengths of 1.973(4) Å to the oxygen and 2.003(5) Å to the nitrogen atom and to one nitrogen atom at 2.028(5) Å of a monodentate 4,4′-bipyridyl ligand. The angle between the two pyridine rings of the 4,4′-bipyridine is 35.3(2)°. The N2O2 equatorial plane, which is planar with an r.m.s. deviation of 0.002 Å, is completed by a water molecule at 2.026(4) Å. Cu(2) is 0.176(2) Å from this plane in the direction of O(19), an atom from a picolinate bonded to Cu(1), which is in an axial position with a bond length of 2.237(3) Å, significantly longer than the equatorial bonds. Thus, the two cop-

per atoms are joined by a *syn–anti*, axial–equatorial carboxylate bridge. There is a weakly bound perchlorate oxygen atom O(71) at 2.756(4) Å in the other axial position.

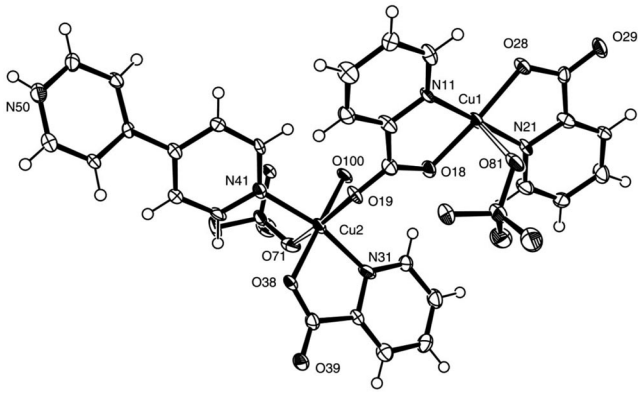

Figure 1. The structure of **1** with ellipsoids at 50% probability. The weak Cu–O(perchlorate) bonds are shown as open lines. Hydrogen atoms on O(100) were not located.

Table 1. Dimensions (Å) and angles (°) in the metal coordination spheres.

Cu(1)–O(18)	1.947(4)
Cu(1)–N(21)	1.966(5)
Cu(1)–O(28)	1.977(4)
Cu(1)–N(11)	1.979(4)
Cu(1)–O(81)	2.546(4)
Cu(2)–O(38)	1.973(4)
Cu(2)–N(31)	2.003(5)
Cu(2)–N(41)	2.028(5)
Cu(2)–O(100)	2.026(4)
Cu(2)–O(19)	2.237(4)
O(18)–Cu(1)–N(21)	95.83(17)
O(18)–Cu(1)–O(28)	172.65(16)
N(21)–Cu(1)–O(28)	83.82(17)
O(18)–Cu(1)–N(11)	84.99(16)
N(21)–Cu(1)–N(11)	175.49(18)
O(28)–Cu(1)–N(11)	95.94(16)
O(18)–Cu(1)–O(81)	97.85(14)
N(21)–Cu(1)–O(81)	91.43(16)
O(28)–Cu(1)–O(81)	89.50(14)
N(11)–Cu(1)–O(81)	84.06(16)
O(38)–Cu(2)–N(31)	82.47(17)
O(38)–Cu(2)–N(41)	87.97(17)
N(31)–Cu(2)–N(41)	166.80(18)
O(38)–Cu(2)–O(100)	169.28(15)
N(31)–Cu(2)–O(100)	93.33(17)
N(41)–Cu(2)–O(100)	94.47(17)
O(38)–Cu(2)–O(19)	98.82(15)
N(31)–Cu(2)–O(19)	100.76(17)
N(41)–Cu(2)–O(19)	89.65(16)
O(100)–Cu(2)–O(19)	91.65(14)

One of the most striking features of this coordination material is the remarkable anion–π interaction with the heterocyclic bipyridine ring (Figure 2). Only the O(74) atom of the ClO_4^- anion is involved in anion–π interactions. O(74) resides above the bridging bipyridine ring (Figure 2), where the distance between the centroid of this ring and the oxygen atom is 3.12 Å. The angle of the O(74)···centroid axis to the plane of the ring is 84.43°, which is close to the ideal value of 90° and thus indicative of strong anion–π interactions. Another interesting feature of this complex is the l.p.–π associations. The contacts are observed between the carbonyl oxygen atom O(39) and the protonated bipyridine ring. The distance between the ring centroid and oxygen (O39) atom is 3.28 Å. This O(l.p.)···π separation is in the range of the few experimental examples so far reported.[7,16] The angle θ (which corresponds to the angle between the O, the ring centroid and the aromatic plane) is 86.70°, reflecting a significant l.p.–π interaction between the two entities. Each molecule of **1** interacts with four neighbouring molecules by means of two anion–π and two O(l.p.)···π contacts to generate a two-dimensional network and these are illustrated in Figures 2 and 3, respectively. Another two-dimensional sheet is loosely formed by three distinct pyr-

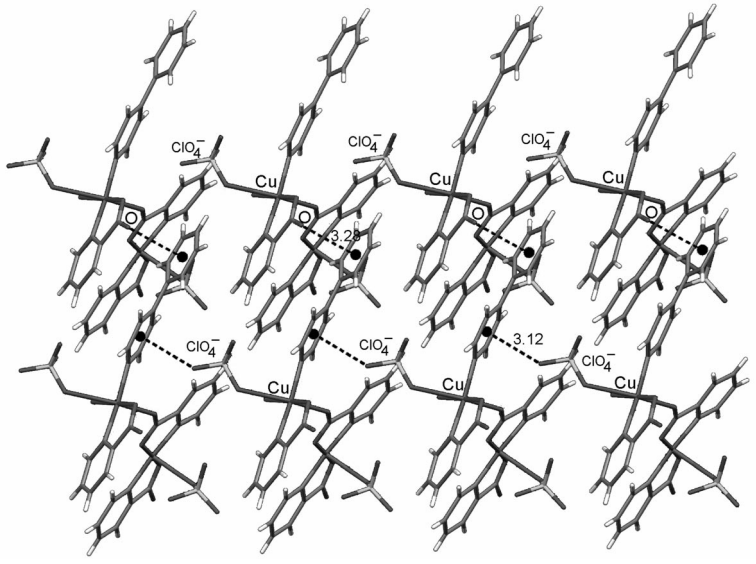

Figure 2. Crystal packing of **1** showing the supramolecular two-dimensional sheet generated from anion–π and l.p.–π interactions. The anion–π interactions and l.p.–π associations are shown as dashed lines; whereas the black spots are the centres of the aromatic rings.

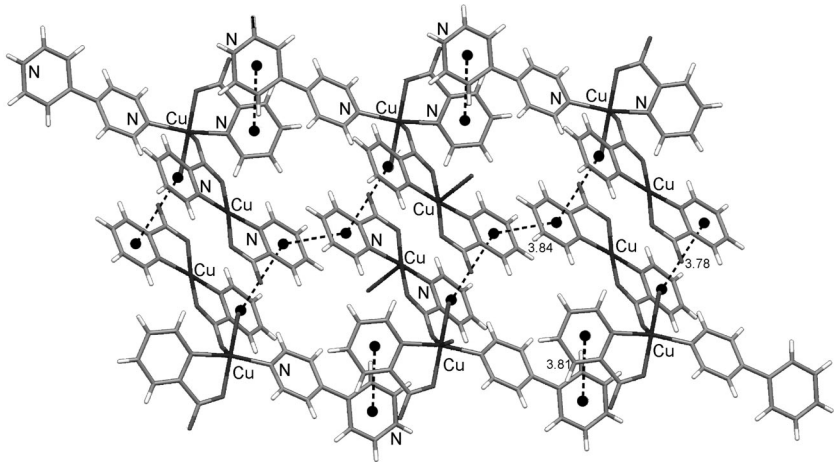

Figure 3. The 2D sheet formed by π–π interactions shown by dashed lines and black spots are the centres of the aromatic rings. The ClO_4^- anions are omitted for clarity.

Table 2. π–π Interactions in complex **1**.

Ring (i)→ring (j)[a]	Dihedral angle (i,j) [°]	Slip angle (i,j) [°]	Distance of centroid (i) from ring (j) [Å]	Distance between the (i,j) ring centroids [Å]
R(1) → R(2)^{iii} [b]	7.84	27.90	3.344	3.783(3)
R(2) → R(2)^{iv} [b]	0.00	26.22	3.448	3.843(3)
R(3) → R(4)^{v} [b]	3.43	21.14	3.539	3.891(3)

[a] Ring numbers are shown in Scheme 1. [b] Symmetry element: iii: 1 – *x*, –*y*, –*z*, iv: 1 – *x*, –1 – *y*, –*z*, v: *x*, 1 + *y*, *z*.

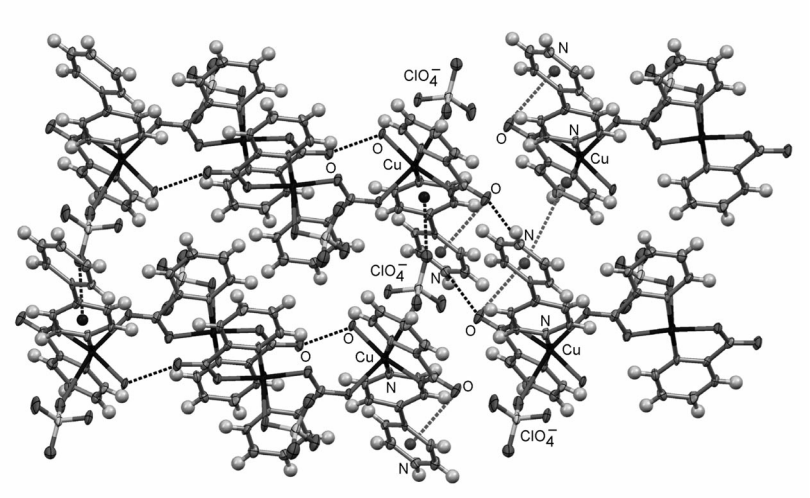

Figure 4. Three-dimensional molecular assembly of complex **1** by π–π, anion–π and l.p.–π binding contacts. H-bonds and anion–π interactions are shown as black dashed lines; however l.p.–π and π–π are shown as grey dashed lines.

idine π–π interactions [centroid-to-centroid distances 3.78, 3.84 and 3.89 Å] (Table 2, Figure 3).

The water molecule forms a strong intermolecular hydrogen bond to O(29) (1 – *x*, –*y*, –*z*) at 2.693(4) Å. To maintain electrical neutrality, N(50) must be protonated and this is confirmed by the formation of bifurcated hydrogen bonds to O(39)^{i} [i: 2 – *x*, 1 – *y*, 1 – *z*] at 2.792(5) Å and with O(72)^{ii} [ii: 1 + *x*, 1 + *y*, *z*] at 3.080(6) Å (Figure 4) to form a two-dimensional extended hydrogen-bonding structure along the (110) direction. Thus the molecules of **1** are assembled by π–π, anion–π, l.p.–π and H-bonding contacts to generate a three-dimensional network (Figure 4).

Theoretical Study

The utilisation of quantum chemical calculations on model systems is an ideal link between theory and experi-

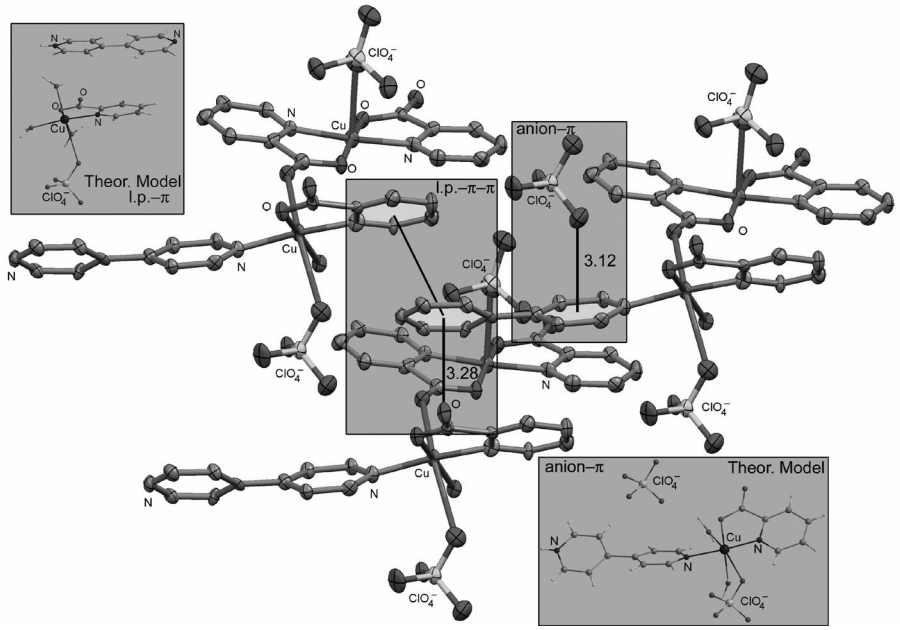

Figure 5. Crystal packing of **1** where the noncovalent interactions and the theoretical models are highlighted. Hydrogen atoms are omitted in the main diagram for clarity.

ment. In this manuscript we have focused our theoretical study on two different aspects. First, we have used AIM theory directly on the experimental structure through single-point calculations by means of DFT calculations to describe the noncovalent interactions. This methodology has been successfully used by Gamez and collaborators to characterise similar interactions on very interesting X-ray structures.[17a,18] Second, we have analysed the effect of the protonation on one of the pyridine rings of bipyridine and also the coordination of a transition metal to the nitrogen atom of pyridine upon the π-acidity of the ring in a small model system.

In Figure 5 we represent a partial view of the packing of the X-ray structure. In the representation the noncovalent interactions are highlighted. In addition we show the theoretical models we have chosen to carry out the theoretical investigation on the anion–π (bottom right corner) and l.p.–π (top left corner) interactions using the AIM method. In Figure 6 we show the results of AIM analysis of the anion–π model of the crystal structure in order to characterise the noncovalent interaction between the ClO_4^- anion and the aromatic rings: anion–π and hydrogen-bonding interactions. Two important conclusions can be drawn from the results. First, there is a bond critical point between one oxygen atom of the anion and one acidic hydrogen atom of the protonated pyridine ring that characterises the hydrogen bond. Second, there are several critical points that connect another oxygen atom of the anion and the pyridine ring that is coordinated to the Cu atom. One important aspect here is the presence of a cage critical point (black circle) that connects the oxygen atom of the ClO_4^- with the centre of the aromatic ring. The cage critical point has been used to characterise the anion–π interaction in many systems and the value of the density has been used as a measure of the bond order.[19] The value of the Laplacian at the critical points is positive, indicating a closed-shell interaction, as is common in noncovalent interactions. In Figure 6 (top left corner), we also show the on-top representation of the distribution. It can be observed that the bond critical points (white circles) connect the oxygen atom with one carbon and one nitrogen atom of the ring, with critical points labelled as BCP_1 and BCP_2, respectively. In addition, two ring critical points (grey circle) connect (RCP_1 and RCP_2) the oxygen atom with the middle of two C–C bonds of the ring. Finally, the interaction is further described by the cage critical point that connects the oxygen atom with the centre of the ring.

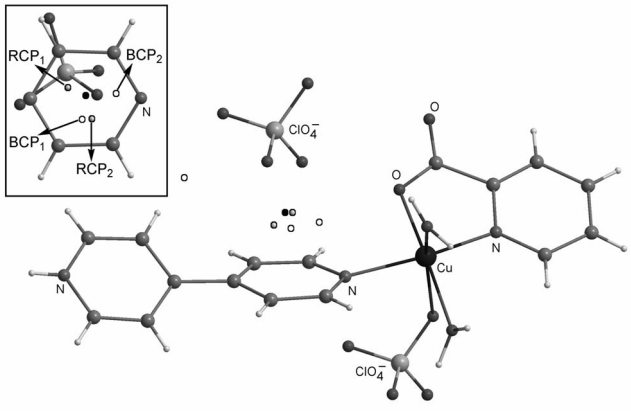

Figure 6. Schematic representation of the distribution of the critical points that connect the anion with the ligand in the theoretical model we have used to evaluate the anion–π interaction. White circles represent the bond critical points, grey circles represent the ring critical points and black circles represent the cage critical points. An on-top view is represented in the left-upper corner.

We have also focused our research on the study of the l.p.–π interaction present in this system by means of the AIM analysis. Experimental proofs for carbonyl–π interactions, and more generally for l.p.–π interactions, are scarce in the literature.[7,17a,20] Crystal structures retrieved from the Cambridge Structural Database (CSD) revealed the occurrence of carbonyl–π interactions in proteins,[7,21] as well as in some other organic crystals including polyacrylate derivatives supported on silica.[22] In an excellent review, Egli and Arkhel have investigated the different possible orientations of a carbonyl group over the interacting π-face of aromatic rings.[7] Three possibilities are operative: (i) the carbonyl may be stacked onto the plane of the ring, (ii) the carbonyl may form an acute angle $0° < \alpha < 90°$ with the ring plane or (iii) the carbonyl may be perpendicular to the ring plane. Likewise, anion···π and carbonyl···π interactions are expected to be energetically favourable in the case of electron-deficient aromatic rings and destabilising for electron-rich rings.[20] As mentioned above, we have used a model of the crystal structure to perform the AIM analysis (see Figure 5). The distribution of critical points is shown in Figure 7. It can be observed that several critical points characterise the l.p.–π interaction. One bond critical point (BCP) connects the oxygen atom of the carboxylate group with one carbon atom of the ring. Two ring critical points connect the oxygen atom with the middle of one C–C and one C–N bond; critical points are labelled as RCP_1 and RCP_2, respectively. Finally the interaction is characterised by a cage critical point that connects the oxygen atom with the centre of the ring.

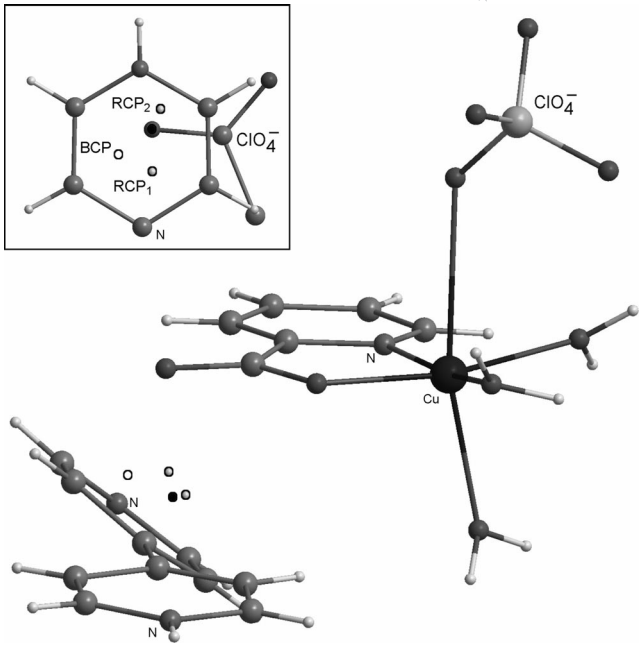

Figure 7. Schematic representation of the distribution of the critical points that connect the lone pair (l.p.) with the ligand in the theoretical model we have used to evaluate the l.p.–π interaction. White circles represent the bond critical points, grey circles represent the ring critical points and black circles represent the cage critical points. An on-top view is shown in the upper left corner.

Once we had characterised the anion–π and l.p.–π interactions present in the crystal structure of **1**, which are responsible for the formation of a 3D supramolecular network, we extended our theoretical study to small models which can be treated at a higher level of theory. We have used these models to study a double effect. A careful analysis of the anion–π interaction present in **1** reveals that the pyridine ring that interacts with the ClO_4^- anion is coordinated to a transition metal (Cu) using the nitrogen atom and it is also bonded in *para* position to a protonated pyridine (bipyridine moiety). Therefore, there are two effects that enhance the π-acidity of the pyridine ring and, consequently, enhance the anion–π interaction. On one hand is the effect of the protonated pyridine, which can be considered as a strong electron-withdrawing group. On the other hand is the effect of having a transition metal coordinated to the nitrogen atom. In order to gain insight into these two effects, we have performed high-level ab initio calculations (RI-MP2/aug-cc-pVTZ) on the systems present in Figure 8 (**2**–**7**). As a model of a transition metal we have used silver and we have used chloride as the counterion of Ag^I in order to keep the model neutral, allowing direct comparisons between complexes **2**–**5** (neutral), and complexes **6** and **7** (charge = +1). The silver atom is expected to have a similar electron-withdrawing effect to copper. As the coordination number of silver is smaller than copper, we have used silver instead of copper in order to keep the size of the system computationally affordable. We have previously shown[23] that pyridine interacts with anions through the hydrogen atoms of the ring and that it does not form stable anion–π complexes. As a matter of fact, for complex **2** the anion–π complex as represented in Figure 8 is not found on the potential hypersurface. Instead, it converges to the geometry depicted in Figure 9. However, when the pyridine is coordinated to Ag, it forms a stable anion–π complex with Cl^- (complex **3**). The computed interaction energies and geometric features of complexes **2**–**7** at the RI-MP2/TZVP//RI-MP2/aug-cc-pVTZ level of theory are summarised in Table 3. The interaction energies of **2** and **3** are –11.57 and –17.27 kcal/mol, respectively. This indicates that the Ag^I atom coordinated to the pyridine has a strong effect on the π-acidity of the ring. A similar finding is obtained by comparing the energetic and geometric features of complexes **4** and **5**. Even in the presence of a hydrogen bond, the coordination of the transition metal in **5** represents a stabilisation of 14 kcal/mol in comparison to **4**. In addition the anion–π interaction distance decreases and the hydrogen bond length increases considerably in **5** compared to **4**. A very interesting result is obtained by comparing the energetic and geometric features of complexes **6** and **7**. Protonation of one of the pyridine rings of bipyridine enhances the π-acidity of both the rings as well as the H-bonding ability because of the positive charge. Consequently complexes **6** and **7** are considerably stabilised. The binding energy of complex **6** is –93.89 kcal/mol and that computed for **7** is –94.66 kcal/mol, indicating that the presence of the transition metal has a positive effect on the anion–π interaction

even in a systemwhere the attractive interaction is dominated by strong electrostatic effects because of the ion-pair nature of the binding. The analysis of the equilibrium distances is also interesting. The global minimum in both structures involves hydrogen bonding of the anion with one acidic hydrogen atom of the protonated pyridine, which is also observed in the crystal structure of **1**. However, in complex **7**, where the transition metal is present, the hydrogen bond length increases and the anion–π distance decreases in comparison to **6**, indicating a strengthening of the anion–π interaction and a weakening of the H-bonding interaction. Finally, the hydrogen bond length in protonated complexes **6** and **7** is considerably shorter than that computed in neutral complexes **4** and **5**, indicating that the hydrogen atom that participates in the interaction has increased acidity due to the positive charge. This indicates that neutral complex **5** has a shorter anion–π interaction distance than **7**.

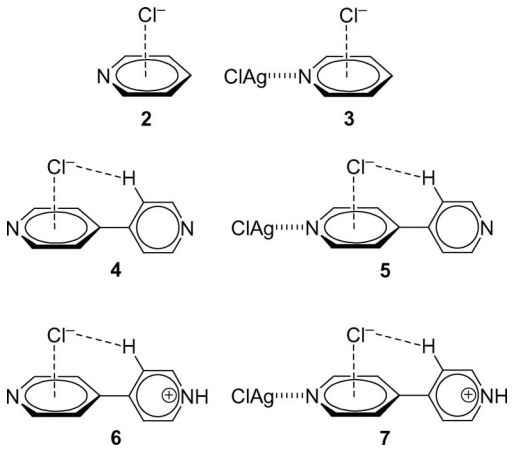

Figure 8. Model complexes **2**–**7**.

Table 3. Interaction energies without and with the basis set superposition error (E and E_{CP}, respectively) computed at the RI-MP2/aug-cc-pVTZ//RI-MP2/TZVP level of theory (kcal/mol) and equilibrium distances from the anion to the ring centroid and to the hydrogen atom (R_e and R_{HB}, respectively, given in Å) computed for complexes **2**–**7**.

Complex	E	E_{CP}	R_e	R_{HB}
2	–12.47	–11.57	2.18	–
3	–18.44	–17.27	3.08	–
4	–14.85	–13.41	3.47	2.31
5	–29.10	–27.35	3.18	2.39
6	–97.47	–93.89	3.55	1.95
7	–96.77	–94.66	3.29	2.00

Conclusions

Several favourable intermolecular forces are responsible for supramolecular self-assemblies. Hydrogen bonding and aromatic π-stacking are widely studied and recognised supramolecular interactions that are involved in the creation of complicated architectures, such as DNA. Understanding these noncovalent bonds is very important for the rational design of noteworthy scaffolds. In this article, a metal-organic compound has been prepared that possesses all func-

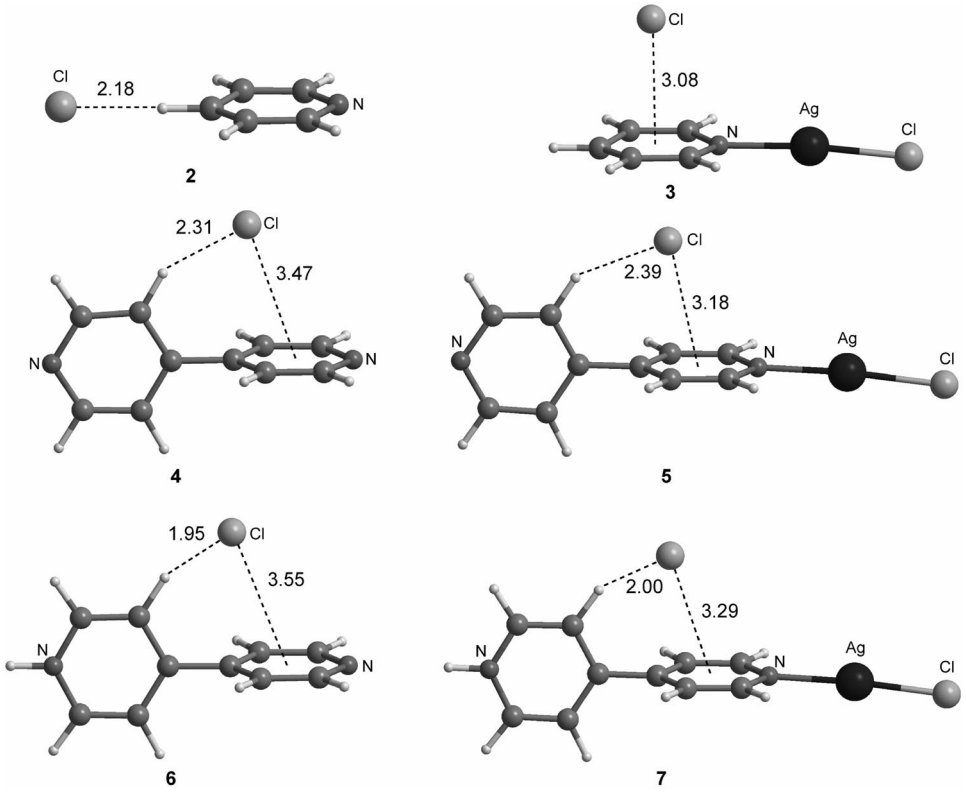

Figure 9. RI-MP2/TZVP optimised structures **2**–**7** (distances are given in Å).

tional groups required to favour supramolecular self-assembly by the coordination of protonated 4,4′-bipyridine and 2-picolinate, and is X-ray characterised. Its solid-state structure demonstrates the generation of 3D networks by noncovalent interactions. Indeed, the X-ray structure of **1** reveals the presence of H bonding and π–π contacts. In addition, this compound shows carbonyl l.p.···π interactions, which contribute to the creation of supramolecular assemblies showing remarkable lone-pair–π/π–π and hydrogen-bonding/anion–π patterns. Theoretical investigations based on the DFT calculations and on AIM analysis support the experimental findings of an intricate intermolecular interaction network that characterises the studied complex. In addition, the effect of the protonation and transition-metal coordination to a bipyridine and a protonated bipyridine system has been studied using high-level ab initio calculations and indicates that both the protonation and transition metal have an important role influencing the π-binding properties of the aromatic ring.

Experimental Section

Starting Materials: The reagents and solvents used were of commercially available reagent quality unless otherwise stated.

Caution! Perchlorate salts of metal complexes with organic ligands are potentially explosive. Only a small amount of material should be prepared and it should be handled with care.

Physical Measurements: Elemental analyses (C, H and N) were performed using a Perkin–Elmer 240C elemental analyser. IR spectra in KBr (4500–500 cm^{-1}) were recorded with a Perkin–Elmer RXI FTIR spectrophotometer. Electronic spectra in the solid state (1000–250 nm) were recorded with a Hitachi U-3501 spectrophotometer.

Synthesis of $[Cu_2(pic)_3(Hbyp)(H_2O)(ClO_4)_2]$ (1): A methanol (5 mL) solution of 2-picolinilic acid (0.37 g, 3 mmol) was added to a solution of copper(II) perchlorate hexahydrate, $Cu(ClO_4)_2{\cdot}6H_2O$ (0.74 g, 2 mmol) in methanol (20 mL) followed by the addition of a methanol solution (5 mL) of 4,4′-bipyridine (1 mmol, 0.156 g). An aqueous solution of perchloric acid (5%) was added dropwise to this mixture to bring the pH of the solution to about 2 with constant stirring. The resulting suspension was put under reflux for 1 h, then cooled and filtered to remove a small amount of bis(2-picolinate)copper(II) dihydrate. The dark blue solution was left at room temperature. Blue single-crystals suitable for X-ray diffraction were obtained by slow evaporation of the mother liquor for several days.

Complex 1: Yield 0.364 g (42%). $C_{28}H_{23}Cl_2Cu_2N_5O_{15}$ (867.50): calcd. C 38.77, H 2.67, N 8.07; found C 38.52, H 2.39, N 7.75. UV/Vis (solid, reflectance): λ_{max} = 675 nm. IR: $\nu_{as}(COO^-)$ = 1638, $\nu_s(COO^-)$ = 1374, and $\nu(ClO_4^-)$ = 1107 cm^{-1}. λ_{max} (solid, reflectance): 675 nm.

Crystal Data Collection and Refinement: A total of 8818 independent reflections were collected with Mo-K_α radiation using the Oxford Diffraction X-Calibur CCD System. The crystal was positioned 50 mm from the CCD. 321 frames were measured with a counting time of 10 s. Data analysis was carried out with the Crysalis program.[24] The structure was solved by direct methods with the SHELX-97 program.[25] The non-hydrogen atoms were refined with anisotropic thermal parameters. The hydrogen atoms bonded to carbon and nitrogen were included in geometric positions and given thermal parameters equivalent to 1.2 times those of the atom to which they were attached. The hydrogen atoms on the water molecule could not be located. An absorption correction was carried out using the ABSPACK program.[26] The structure was refined on F^2 using SHELX-97[25] to R_1 = 0.0770 and wR_2 = 0.1797 for 3936 reflections with $I > 2\sigma(I)$. Crystallographic data in CIF format for the structures are reported. Details of crystallographic data and refinements of the complexes are summarised in Table 4.

Table 4. Summary of crystallographic data for complex **1**.

	1
Empirical formula	$C_{28}H_{23}Cl_2Cu_2N_5O_{15}$
Formula mass	867.49
Crystal system	triclinic
Space group	$P\bar{1}$ (no. 2)
a [Å]	8.3371(16)
b [Å]	10.0222(18)
c [Å]	19.786(4)
α [°]	93.629(15)
β [°]	98.961(16)
γ [°]	92.417(15)
V [Å^3]	1627.5(5)
Z	2
D_{calcd} [g cm^{-3}]	1.766
μ [mm^{-1}]	1.553
R [$I > 2\sigma(I)$]	0.0769
Temperature [K]	150

CCDC-709084 (for **1**) contains the supplementary crystallographic data for this paper. These data can be obtained free of charge from The Cambridge Crystallographic Data Centre via www.ccdc.cam.ac.uk/data_request/cif.

Theoretical Calculations: The geometries of complexes **2**–**7** studied in this work were fully optimised at the RI-MP2/TZVP level of theory using the Turbomole program.[27] These geometries were used to perform single-point calculations using the augmented correlation-consistent polarised valence triple-ζ (aug-cc-pVTZ) basis set in order to obtain more accurate energetic values. For the silver atom the calculations were performed using a relativistic effective core potential (ECP28MWB).[28] The binding energies were calculated with corrections for the basis set superposition error (BSSE) using the Boys–Bernardi counterpoise technique.[29] The RI-MP2 method applied to the study of anion–π interactions is considerably faster than the MP2 and the interaction energies and equilibrium distances are almost identical for both methods.[8c,30] The topological analysis of the electron charge density performed for the theoretical models of the crystal structure was determined using Bader's theory of "atoms in molecules" (AIM).[31] The electronic density analysis was performed using the AIM2000 program[32] at the B3LYP/6-31++G** level of theory. The wave function was obtained using the Gaussian-03 program.[33] As in previous studies,[34] the AIM theory was performed directly on experimental structures by single-point calculations to estimate the intermolecular interactions. AIM is based upon those critical points where the gradient of the density, $\nabla\rho$, vanishes. In particular, two bonded atoms are connected with a bond path through the bond critical point. Importantly, the electron density at the bond critical points roughly correlates with the strength of chemical bonds and interactions.[17,32]

Acknowledgments

Chaitali Biswas is thankful to the University Grants Commitee (UGC), India for research fellowships [Sanction no. UGC/29/Jr. Fellow(Sc.) 05-06]. We also thank the British Engineering and Physical Sciences Research Council (EPSRC) and the University of Reading for funds for the X-Calibur system.

[1] D. T. Bowron, J. L. Finney, A. K. J. Soper, *J. Am. Chem. Soc.* **2006**, *128*, 5119–5126.
[2] a) D. N. Reinhoudt, M. Crego-Calama, *Science* **2002**, *295*, 2403–2407; b) A. L. Maksimov, D. A. Sakharov, T. Y. Filippova, A. Y. Zhuchkova, E. A. Karakhanov, *Ind. Eng. Chem. Res.* **2005**, *44*, 8644–8653; c) J. W. Bell, N. M. Hext, *Chem. Soc. Rev.* **2004**, *33*, 589–598.
[3] C. J. Janiak, *J. Chem. Soc., Dalton Trans.* **2000**, 3885–3896.
[4] J.-M. Lehn, J. L. Atwood, J. E. D. Davies, D. D. MacNicol, F. Vögtle (Eds.), *Comprehensive Supramolecular Chemistry*, Pergamon, Oxford, UK, **1996**.
[5] a) M. Nishio, M. Hirota, Y. Umezawa, *The C–H···π Interactions (Evidence, Nature and Consequences)*, Wiley-VCH, New York, **1998**; b) J. C. Ma, D. A. Dougherty, *Chem. Rev.* **1997**, *97*, 1303–1324.
[6] P. Gamez, T. J. Mooibroek, S. J. Teat, J. Reedijk, *Acc. Chem. Res.* **2007**, *40*, 435–444.
[7] a) M. Egli, S. Arkhel, *Acc. Chem. Res.* **2007**, *40*, 197–205; b) T. J. Mooibroek, P. Gamez, J. Reedijk, *CrystEngComm* **2008**, *10*, 1501–1515.
[8] a) O. B. Berryman, V. S. Bryantsev, D. P. Stay, D. W. Johnson, B. P. Hay, *J. Am. Chem. Soc.* **2007**, *129*, 48–58; b) C. Garau, A. Frontera, D. Quiñonero, P. Ballester, A. Costa, P. M. Deyà, *Chem. Phys. Lett.* **2004**, *392*, 85–101; c) D. Quiñonero, C. Garau, A. Frontera, P. Ballester, A. Costa, P. M. Deyà, *J. Phys. Chem. A* **2005**, *109*, 4632–4637; d) D. Kim, P. Tarakeshwar, K. S. Kim, *J. Phys. Chem. A* **2004**, *108*, 1250–1258.
[9] Y. S. Rosokha, S. V. Lindeman, S. V. Rosokha, J. K. Kochi, *Angew. Chem. Int. Ed.* **2004**, *43*, 4650–4652.
[10] H. J. Schneider, F. Werner, T. Blatter, *J. Phys. Org. Chem.* **1993**, *6*, 590–594.
[11] a) A. Frontera, F. Saczewski, M. Gdaniec, E. Dziemidowicz-Borys, A. Kurland, P. M. Deyà, D. Quiñonero, C. Garau, *Chem. Eur. J.* **2005**, *11*, 6560–6567; b) M. Mascal, *Angew. Chem. Int. Ed.* **2006**, *45*, 2890–2893.
[12] a) B. L. Schottel, H. T. Chifotides, M. Shatruk, A. Chouai, L. M. Pérez, J. Bacsa, K. R. Dunbar, *J. Am. Chem. Soc.* **2006**, *128*, 5895–5912; b) C. Garau, D. Quiñonero, A. Frontera, A. Costa, P. Ballester, P. M. Deya, *Chem. Phys. Lett.* **2003**, *370*, 7–13.
[13] a) P. U. Maheswari, B. Modec, A. Pevec, B. Kozlevčar, C. Massera, P. Gamez, J. Reedijk, *Inorg. Chem.* **2006**, *45*, 6637–6645; b) H. Casellas, C. Massera, F. Buda, P. Gamez, J. Reedijk, *New J. Chem.* **2006**, *30*, 1561–1566; c) C. Garau, D. Quiñonero, A. Frontera, P. Ballester, A. Costa, P. M. Deyà, *J. Phys. Chem. A* **2005**, *109*, 9341–9345; d) M. Mascal, A. Armstrong, M. D. Bartberger, *J. Am. Chem. Soc.* **2002**, *124*, 6274–6276.
[14] S. Scheiner, T. Kar, J. Pattanayek, *J. Am. Chem. Soc.* **2002**, *124*, 13257–13264.
[15] R. F. W. Bader, *J. Phys. Chem. A* **1998**, *102*, 7314–7323.
[16] Z. Lu, P. Gamez, I. Mutikainen, U. Turpeinen, J. Reedijk, *Cryst. Growth Des.* **2007**, *7*, 1669–1671.
[17] a) M. P. Waller, A. Robertazzi, J. A. Platts, D. E. Hibbs, P. A. Williams, *J. Comput. Chem.* **2006**, *27*, 491–504; b) A. R. Pirek, A. T. Dubis, S. J. Grabowskiand, N. Modranka, *Chem. Phys.* **2006**, *320*, 247–258.
[18] R. J. Götz, A. Robertazzi, I. Mutikainen, U. Turpeinen, P. Gamez, J. Reedijk, *Chem. Commun.* **2008**, 3384–3386.
[19] a) D. Quiñonero, C. Garau, A. Frontera, P. Ballester, A. Costa, P. M. Deyà, *Chem. Phys. Lett.* **2002**, *359*, 486–492; b) C. Garau, A. Frontera, D. Quiñonero, P. Ballester, A. Costa, P. M. Deyà, *ChemPhysChem* **2003**, *4*, 1344–1348.
[20] a) J. E. Gautrot, P. Hodge, D. Cupertinob, M. Helliwella, *New J. Chem.* **2006**, *30*, 1801–1807; b) T. J. Mooibroek, S. J. Teat, C. Massera, P. Gamez, J. Reedijk, *Cryst. Growth Des.* **2006**, *6*, 1569–1574.
[21] a) K. A. Thomas, G. M. Smith, T. B. Thomas, R. J. Feldmann, *Proc. Natl. Acad. Sci. USA* **1982**, *79*, 4843–4847; b) C.-Y. Kim, P. P. Chandra, A. Jain, D. W. Christianson, *J. Am. Chem. Soc.* **2001**, *123*, 9620–9627.
[22] A. Gambaro, P. Ganis, F. Manoli, A. Polimeno, S. Santi, A. Venzo, *J. Organomet. Chem.* **1999**, *583*, 126–130.
[23] D. Quiñonero, A. Frontera, P. M. Deyà, *ChemPhysChem* **2008**, *9*, 397–399.
[24] *Crysalis*, v1, Oxford Diffraction Ltd., Oxford, UK, **2005**.
[25] G. M. Sheldrick, *SHELXL-97*, University of Göttingen, Göttingen, Germany, **1997**.
[26] ABSPACK, Oxford Diffraction Ltd., Oxford, UK, **2005**.
[27] R. Ahlrichs, M. Bär, M. Häser, H. Horn, C. Kölmel, *Chem. Phys. Lett.* **1989**, *162*, 165–169.
[28] A. Niklass, M. Dolg, H. Stoll, H. Preuss, *J. Chem. Phys.* **1995**, *102*, 8942–8952.
[29] S. B. Boys, F. Bernardi, *Mol. Phys.* **1970**, *19*, 553–566.
[30] D. Quiñonero, C. Garau, A. Frontera, P. Ballester, A. Costa, P. M. Deyà, *J. Phys. Chem. A* **2006**, *110*, 5144–5157.
[31] a) R. F. W. Bader, *Chem. Rev.* **1991**, *91*, 893; b) R. F. W. Bader, *Atoms in Molecules. A Quantum Theory*, Clarendon, Oxford, **1990**.
[32] F. B. König, J. Schönbohm, D. Bayles, *J. Comput. Chem.* **2001**, *22*, 545–559.
[33] M. J. Frisch, G. W. Trucks, H. B. Schlegel, G. E. Scuseria, M. A. Robb, J. R. Cheeseman Jr., J. A. Montgomery, T. Vreven, K. N. Kudin, J. C. Burant, J. M. Millam, S. S. Iyengar, J. Tomasi, V. Barone, B. Mennucci, M. Cossi, G. Scalmani, N. Rega, G. A. Petersson, H. Nakatsuji, M. Hada, M. Ehara, K. Toyota, R. Fukuda, J. Hasegawa, M. Ishida, T. Nakajima, Y. Honda, O. Kitao, H. Nakai, M. Klene, X. Li, J. E. Knox, H. P. Hratchian, J. B. Cross, V. Bakken, C. Adamo, J. Jaramillo, R. Gomperts, R. E. Stratmann, O. Yazyev, A. J. Austin, R. Cammi, C. Pomelli, J. W. Ochterski, P. Y. Ayala, K. Morokuma, G. A. Voth, P. Salvador, J. J. Dannenberg, V. G. Zakrzewski, S. Dapprich, A. D. Daniels, M. C. Strain, O. Farkas, D. K. Malick, A. D. Rabuck, K. Raghavachari, J. B. Foresman, J. V. Ortiz, Q. Cui, A. G. Baboul, S. Clifford, J. Cioslowski, B. B. Stefanov, G. Liu, A. Liashenko, P. Piskorz, I. Komaromi, R. L. Martin, D. J. Fox, T. Keith, M. A. Al-Laham, C. Y. Peng, A. Nanayakkara, M. Challacombe, P. M. W. Gill, B. Johnson, W. Chen, M. W. Wong, C. Gonzalez, J. A. Pople, Gaussian 03, Revision C.02, Gaussian Inc., Wallingford, CT, **2004**.
[34] a) S. R. Choudhury, P. Gamez, A. Robertazzi, C.-Y. Chen, H. M. Lee, S. Mukhopadhyay, *Cryst. Growth Des.* **2008**, *8*, 3773–3784; b) C. F. Matta, N. Castillo, R. J. Boyd, *J. Phys. Chem. B* **2006**, *110*, 563–578; c) A. Robertazzi, J. A. Platts, *Chem. Eur. J.* **2006**, *12*, 5747–5757; d) D. E. Hibbs, J. Overgaard, J. A. Platts, M. P. Waller, M. B. Hursthouse, *J. Phys. Chem. B* **2004**, *108*, 3663–3668.

Received: January 30, 2009
Published Online: April 9, 2009

